

Coherent control of terahertz charge oscillations in a coupled quantum well using phase-locked optical pulses

Paul C. M. Planken, Igal Brener, and Martin C. Nuss

AT&T Bell Laboratories, 101 Crawfords Corner Road, Holmdel, New Jersey 07733-3030

Marie S. C. Luo and Shun Lien Chuang

Department of Electrical and Computer Engineering, University of Illinois at Urbana-Champaign, Urbana, Illinois 61801-2991

(Received 23 February 1993)

We demonstrate that we can enhance, weaken, and also phase shift terahertz (THz) radiation emitted by optically excited quantum beats in a coupled quantum well. The changes in the evolution of the THz radiation are induced by exciting the sample with a second optical pulse, phase locked with the first. We observe phase shifts in the emitted THz radiation of 330 fs for a change in the optical-pulse separation of only 1.33 fs.

In optical experiments in gases, liquids, and solids, transient coherent phenomena can take place within the time interval before dephasing of a transition is complete. Such phenomena have been studied in the past using photon echoes, transient gratings, or stimulated Raman scattering. These are mostly four-wave mixing (FWM) techniques, involving the third-order nonlinear susceptibility $\chi^{(3)}$. Although the outcome of these experiments is usually not sensitive to the relative optical phase of the pulses, there are other classes of experiments in which the phase of the second pulse with respect to the phase of the first pulse is important. Then, if the time separation between the two pulses falls within the dephasing time of a transition with which they are resonant, the outcome of the experiment strongly depends on their exact phase difference. For example, pulses with a fixed phase difference have been used in the measurement of the optical coherence decay in sodium gas¹ and iodine,² to observe Ramsey interference fringes in two-photon spectroscopy,³ and to observe the interference between vibrational wave packets in iodine,⁴ all by detecting the intensity of the optical fluorescence between two levels. While most gases and liquids possess a center of inversion symmetry, semiconductor heterostructures can be designed to lack inversion symmetry so that second-order nonlinear optical processes are allowed. This, combined with dephasing times of excitons on the order of a few picoseconds,⁵ has recently allowed the generation of coherent terahertz (THz) radiation emitted from charge oscillations that accompany excitonic quantum beats in such semiconductor structures.^{6,7}

In this paper we combine phase-locked pulse excitation with terahertz generation in semiconductor quantum wells and demonstrate that we can enhance, weaken, and induce *large phase shifts* in *excitonic charge oscillations* in a semiconductor coupled quantum well (CQW) [Fig. 1(a)], simply by adjusting the optical phase difference between two phase-locked optical pulses. Specifically, we induce phase shifts in the emitted THz radiation of as much as 330 fs, for a change in the optical delay of only a few femtoseconds. To our knowledge this is the first experiment in which such large optically induced phase

shifts have been directly observed. This observation is possible because of the nonvanishing nonlinear optical susceptibility $\chi^{(2)}$ in these samples and the time-resolved detection of both the amplitude *and* phase of the resulting terahertz radiation. We describe the amplitude and phase changes as resulting from the interference of the excitonic wave functions excited by the two phase-locked pulses. Alternatively, from a nonlinear optics point of view, the radiation is resonantly generated in our sample by difference-frequency mixing between optical photons, and the observed effects result from the possibility to mix optical photons not only from each of the individual pulses, but also photons belonging to two *different*, temporally separate optical pulses.

The CQW structure [Fig. 1(a)] consists of 10 pairs of a 145-Å GaAs wide well (WW) with a 100-Å GaAs narrow well (NW) separated by a 25-Å $\text{Al}_{0.2}\text{Ga}_{0.8}\text{As}$ barrier. A semitransparent chromium contact is evaporated on top. The sample is mounted in a continuous-flow liquid-helium cryostat and the temperature is kept at 10 K. By

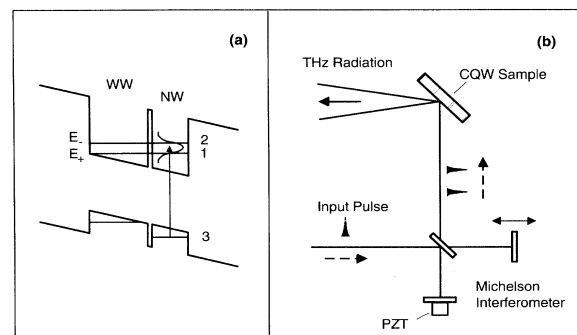


FIG. 1. (a) Energy diagram of the coupled quantum well consisting of a wide well (WW) and a narrow well (NW). 1 and 2 are the bonding and antibonding electron states of the coupled system and 3 is the localized hole state. (b) Schematic of the experimental setup. Two phase-locked pulses from a Michelson interferometer illuminate the CQW sample and generate THz radiation. One of the end mirrors is mounted on a piezoelectric transducer (PZT) to fine tune the optical delay.

adjusting the electric field in the CQW, the $n = 1$ electron levels in the narrow well and the wide well can be aligned. For transitions from the NW, the Coulomb interaction between the electron and the hole downshifts the value of the electric field where the resonance condition is fulfilled to that corresponding to the built-in field, where our experiments are performed. The new excitonic eigenstates of the coupled system consist of a bonding and an antibonding state with an energy separation measured to be 6 meV. For more details on this system we refer the reader to Ref. 6.

Our experimental setup [Fig. 1(b)] uses 80 fs, 15 nJ pulses from a mode locked, 82-MHz repetition rate, argon-ion pumped Ti:sapphire laser, tunable around 800 nm. The laser beam is split in two. One beam is sent into a Michelson interferometer setup. The arms of the Michelson can be set at different delays so that the pulses emerging from the interferometer are separated in time. One of the end mirrors of the Michelson is also mounted onto a piezoelectric transducer (PZT) to actively stabilize the length of the arm to within a fraction of a wavelength. The pulse pair that emerges from the Michelson is weakly focused onto the quantum well sample with its polarization in the plane of incidence. The laser is tuned to the NW interband transitions and we typically excite a carrier density of less than 10^{10} cm^{-2} . The bandwidth of the laser is larger than the energy splitting between the bonding and antibonding exciton eigenstates of the CQW and we coherently excite them both. The generated THz beam is detected with a $50\text{-}\mu\text{m}$ photoconducting dipole antenna⁸ with a hyperhemispherical silicon substrate lens. The antenna is gated by the second laser beam. By measuring the photocurrent from the antenna versus the delay between the gating pulse and the THz signal, we measure the electric field $E(t)$ of the signal. For a given overall delay between the two optical pulses, we measure the THz signals for several values of the optical phase difference Φ between the two pulses by fine tuning the delay with the PZT.

Detected THz wave forms for several values of the phase difference Φ between the two pulses at an overall separation of $\tau = 2T_{12} \equiv 2|2\pi/\omega_{12}|$ [with $\omega_{12} = (E_1 - E_2)/\hbar$], corresponding to two oscillation periods of the emitted THz radiation, are plotted in Fig. 2. The upper two traces are the individual THz wave forms generated by the second and first optical pulse, respectively. The other traces result when *both* pulses illuminate the sample. From the figure we can see that for a phase difference of $\Phi = 0$ the arrival of the second optical pulse amplifies the emitted THz radiation more than 3 times. On the other hand, when we adjust for a phase difference of $\Phi = \pi$, the second pulse effectively terminates the THz radiation.

The results are markedly different when the separation between both optical pulses is not an integer multiple of the THz oscillation period. In Fig. 3 we plot the detected THz wave forms for several values of the phase difference between the two pulses, for an overall delay of $\tau = 2.5T_{12}$. Again the upper two curves represent the THz signals generated by the individual pulses. When both pulses arrive at the sample with $\Phi = 0$, we measure a slight in-

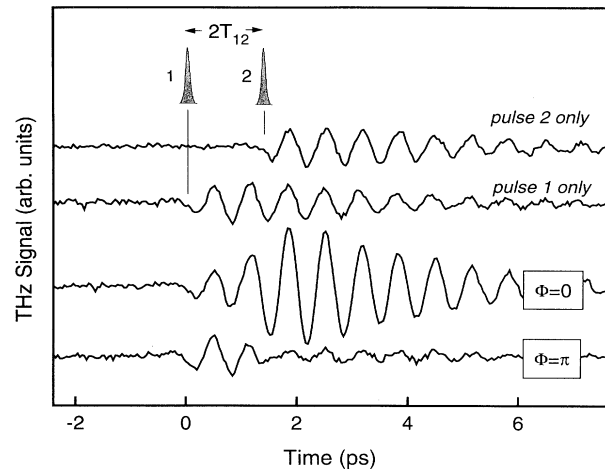


FIG. 2. Measured THz wave forms. The upper two curves are generated by each pulse individually. The lower two are generated by the phase-locked pulse pair for a time separation of two oscillation periods of the THz radiation, and correspond to two different values of the optical phase difference Φ . The pulses sketched in the figure show the arrival time of the two optical pulses.

crease in amplitude and a *phase shift* in the emitted THz radiation of $-\pi/2$ as evidenced by a single prolonged oscillation after the arrival of the second pulse. For $\Phi = \pi$ we also observe a slight increase in amplitude, but with a *phase shift* of $+\pi/2$ indicated by a single shortened oscillation after the arrival of the second pulse. Both phase shifts can clearly be identified with the aid of the dashed vertical line in the figure. A weakening of the signal

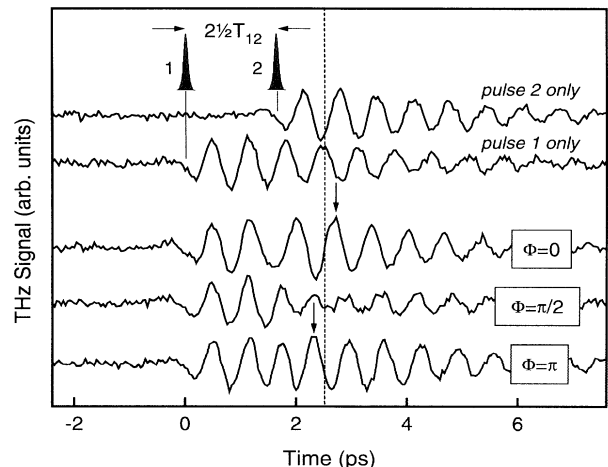


FIG. 3. Measured THz wave forms. The upper two curves are generated by each pulse individually. The lower three are generated by the phase-locked pulse pair for a time separation of two and a half oscillation periods of the THz radiation, and correspond to three different values of the optical difference Φ . The pulses sketched in the figure show the arrival time of the two optical pulses. The vertical arrows and the dashed line are used to emphasize the phase shifts in the emitted radiation.

occurs for $\Phi = \pi/2$. Both the coherent effects in Fig. 3 and the ones shown in Fig. 2 are only observed when the separation between the pulses is less than the time it takes for the THz signal to decay completely. We cannot reproduce them by adding the THz signals from the individual pulses, which would give an increase in amplitude by a factor of 2 for the case of Fig. 2 and no signal at all for the case of Fig. 3.

To understand our observations, we model the exciton transitions in the CQW as a three-level system [Fig. 1(a)]. Charge oscillations result from the time evolution of the coherent superposition of the two excitonic eigenstates of the sample. The charge oscillations give rise to a time-varying dipole moment that radiates at the splitting frequency.^{6,7} The changes in the measured THz signals induced by the second pulse are produced by the *interference* between the coherent superposition of states excited

by the first pulse and the coherent superposition excited by the second pulse. Using the density matrix formulation for the three-level model, the time-dependent far-infrared polarization (or optically rectified signal) associated with the quantum beats, can be written as

$$P_{\text{FIR}}(t) = 2|e| \text{Re}[z_{12}\rho_{12}(t)], \quad (1)$$

with z_{12} being the $1 \rightarrow 2$ intersubband transition-dipole element, and the density matrix element ρ_{12} representing the coherence between the two excitonic levels. The radiated electric field can be written as $E_{\text{FIR}}(t) \propto \partial^2 P_{\text{FIR}} / \partial t^2$. Assuming δ -pulse excitation and writing the electric-field amplitude of the pulse pair as $E_L(t) = E_0 \delta(t) + E_0 e^{i\Phi} \delta(t - \tau)$, an expansion of ρ_{12} to second order in electric field under the rotating-wave approximation yields

$$\rho_{12}^{(2)}(t) = \frac{\mu_{13}\mu_{32}}{\hbar^2} E_0^2 \{ e^{-i\omega_{12}t} \theta(t) + e^{-i\omega_{12}(t-\tau)} \theta(t-\tau) + e^{-i\Phi} e^{-i\omega_{12}(t-\tau)} e^{-i\Delta_{13}\tau} \theta(t-\tau) + e^{i\Phi} e^{-i\omega_{12}(t-\tau)} e^{i\Delta_{23}\tau} \theta(t-\tau) \}, \quad (2)$$

where we have assumed that all relaxation-time constants are infinite. In Eq. (2), $\omega_{12} = \omega_{13} - \omega_{23}$, Φ is the optical phase difference, $\theta(t)$ and $\theta(t - \tau)$ are Heaviside step functions, $\Delta_{13} = \omega_{13} - \Omega_L$ and $\Delta_{23} = \omega_{23} - \Omega_L$ are the frequency detunings of the laser with respect to the $3 \rightarrow 1$ and $3 \rightarrow 2$ transitions, and μ_{13} and μ_{23} are the interband optical transition-dipole moments. The first two terms oscillating at ω_{12} within the curly brackets constitute the response of the system to each optical pulse separately, not taking interference effects into account. The remaining two terms can be viewed as interference terms arising from the coherent addition of the wave functions excited by the pulses. Their value depends on detunings Δ_{13} and Δ_{23} , the overall delay τ between the two pulses, and the optical phase difference Φ . Most features apparent in the measured THz signals are described by Eq. (2). For example, for $\tau = 2.5T_{12}$, $\Phi = 0$, and $\Delta_{13} = -\Delta_{23} = \omega_{12}/2$, the first two terms within the curly brackets cancel, leaving two terms that are phase shifted by $-\pi/2$. For $\tau = 2T_{12}$, $\Phi = 0$, and $\Delta_{13} = -\Delta_{23} = \omega_{12}/2$, all four terms add up constructively and give an increase in amplitude by a factor of 4 (the difference with the measured increase of a factor of approximately 3 is caused by the assumption of infinite dephasing times in the calculation). To incorporate effects of finite laser-pulse duration and dephasing times, we choose to solve the nonlinear optical Bloch equations numerically using a fourth-order Runge-Kutta method. From the calculated $\rho_{12}(t)$ we can obtain the electric field [Eq. (1)] which closely resembles $\rho_{12}(t)$. However, because we do not precisely know the frequency response function of our detector, we directly plot $\text{Re}[\rho_{12}(t)]$. An example is shown in Fig. 4, where we plot the numerical calculations of $\text{Re}[\rho_{12}(t)]$ for several values of Φ at a value of the overall delay $\tau = 2.5T_{12}$ used in the experiment. The calculations nicely reproduce the phase shifts

of $-\pi/2$, $\pi/2$ for $\Phi = 0$, and π , respectively, as well as the weakening of the signal for $\Phi = \pi/2$ that we observe experimentally in Fig. 3. Although not shown here, simulations of $\text{Re}[\rho_{12}(t)]$ for $\tau = 2T_{12}$ are also in excellent agreement with the measured THz wave forms in Fig. 2.

Our measurements and calculations prove that the observed effects measured in the emitted THz radiation must be explained as arising from the (coherent) addition of wave-function amplitudes excited by the two pulses. It is important to note that they *cannot* be understood by

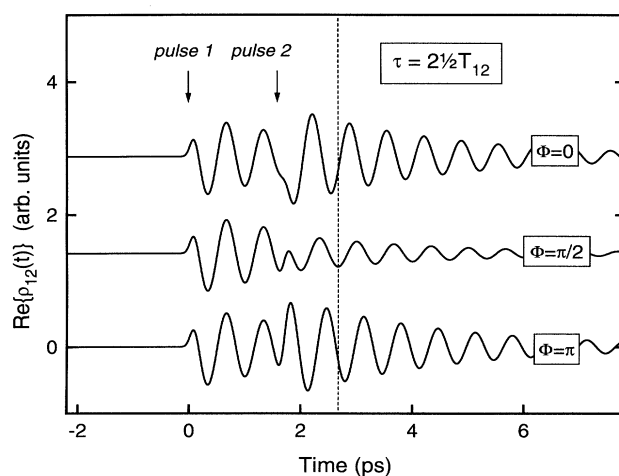


FIG. 4. Numerical calculations of the time dependence of $\text{Re}[\rho_{12}(t)]$ at an overall pulse separation of two and a half THz oscillation periods, for several values of the optical phase difference Φ . Vertical arrows mark the arrival time of the optical pulses. The calculation assumes Gaussian pulses of duration 120 fs and a dephasing time of 2.75 ps. The vertical dashed line is a guide to identify the phase shifts.

comparing the spectral intensity of the phase-locked pulse pair, which shows interference fringes, with the exciton absorption spectrum of our CQW. Although matching the exciton absorption spectrum with the power spectrum of the pulse pair can explain the increase and termination of the THz amplitude for $\tau=2T_{12}$, it *does not explain the phase shifts* in the emitted THz radiation for any other delay. This should not be too surprising, as in comparing the spectral *intensity* of the pulses with the absorption spectrum, phase information is inherently lost.

From a nonlinear optics point of view, the generation of THz radiation from the CQW is a resonant difference-frequency mixing process involving the second-order nonlinear susceptibility $\chi^{(2)}$ of the three-level system. We can look at the four terms in Eq. (2) as the four possibilities for difference-frequency mixing from a pulse pair: mixing can either occur between the optical electric fields belonging to the same pulse or between those of the two pulses that are *separated* in time. The former is always possible, the latter only when the coherent optical polar-

ization stored in the medium by the first pulse has not completely decayed by the time the second pulse arrives.

In conclusion, we have used phase-locked pulse pairs to phase shift, amplify, and suppress THz radiation from charge oscillations. Our coherent detection technique allows us to time-resolve phase shifts in the emitted THz radiation that have not been observed previously. Specifically, we observe a phase shift of 330 fs for a change in the optical pulse separation of only 1.33 fs. These large phase shifts result from interference between the excitonic wave functions set up by the two phase-locked pulses and can be reproduced from the optical Bloch equations of the three-level excitonic system.

We would like to acknowledge the assistance of G. E. Doran and B. Tell in the fabrication of the photoconducting antenna used in the experiments, K. Köhler for providing the sample, and thank D. A. B. Miller and A. M. Weiner for valuable discussions. The work at the University of Illinois was supported by the Office of Naval Research under Grant No. N00014-90-J-1821.

¹J. T. Fourkas, W. L. Wilson, G. Wäckerle, A. E. Frost, and M. D. Fayer, *J. Opt. Soc. Am. B* **6**, 1905 (1989).

²W. S. Warren and A. H. Zewail, *J. Chem. Phys.* **78**, 2279 (1983).

³M. M. Salour and C. Cohen-Tannoudji, *Phys. Rev. Lett.* **38**, 757 (1977).

⁴N. F. Scherer, R. J. Carlson, A. Matro, M. Du, A. J. Ruggiero, V. Romero-Rochin, J. A. Cina, G. R. Fleming, and S. A. Rice, *J. Chem. Phys.* **95**, 1487 (1991).

⁵D. S. Kim, J. Shah, J. E. Cunningham, T. C. Damen, W. Schäfer, M. Hartmann, and S. Schmitt-Rink, *Phys. Rev. Lett.*

68, 1006 (1992); L. Schultheis, A. Honold, J. Kuhl, K. Köhler, and C. W. Tu, *Phys. Rev. B* **34**, 9027 (1986).

⁶H. G. Roskos, M. C. Nuss, J. Shah, K. Leo, D. A. B. Miller, A. M. Fox, S. Schmitt-Rink, and K. Köhler, *Phys. Rev. Lett.* **68**, 2216 (1992).

⁷P. C. M. Planken, M. C. Nuss, I. Brener, K. W. Goossen, M. S. C. Luo, S. L. Chuang, and L. Pfeiffer, *Phys. Rev. Lett.* **69**, 3800 (1992).

⁸P. R. Smith, D. H. Auston, and M. C. Nuss, *IEEE J. Quantum Electron.* **QE-24**, 255 (1988).